

Modeling of Strain Rate Effects in Automotive Impact

Srdan Simunovic and Phani Kumar V. V. Nukala
Oak Ridge National Laboratory

James Fekete
General Motors Corporation

David Meuleman
National Steel Corporation

Marcio Milititsky
DaimlerChrysler Corporation

Copyright © 2003 Society of Automotive Engineers, Inc.

ABSTRACT

This paper deals with the effects of various approaches for modeling of strain rate effects for mild and high strength steels (HSS) on impact simulations. The material modeling is discussed in the context of the finite element method (FEM) modeling of progressive crush of energy absorbing automotive components. The characteristics of piecewise linear plasticity strain rate dependent material model are analyzed and various submodels for modeling of impact response of steel structures are investigated. The paper reports on the ranges of strains and strain rates that are calculated in typical FEM models for tube crush and their dependence on the material modeling approaches employed. The models are compared to the experimental results from drop tower tests.

INTRODUCTION

Strain rate dependency of steels [1], although long recognized and documented as an important effect [2, 3], has been more widely used in crash models only in the past few years [4-6]. Until recently, computational resource limitations dictated a size of the finite elements that could not conform to the detailed features of the vehicle crush. Large finite element sizes made the structures relatively stiff, so that the strain rate dependency was just one of the effects that was obfuscated by the heuristic modeling rules that were shown to give a good correlation with experiments [3]. With the increase in computational power, accompanied

by the increasing FEM mesh density, it became possible for vehicle model components to conform to the actual physical deformation. However, without accounting for the strain rate sensitivity, finely discretized FEM models tend to soften as the element density increases. To counter this softening trend and, moreover, to model the physics of the process more accurately, the strain rate effects must be taken into account. In addition to better representation of the material response, strain rate sensitivity has an added benefit in promoting computational stability of simulations [7]. Pathological FEM mesh sensitivity, so characteristic of modeling of localized deformations, is reduced when strain rate sensitive materials are used. Material rate dependence introduces a length scale that is proportional to the length of propagation of elastic waves. This length scale has a physical character [7, 8] as opposed to the length scale imposed by the element mesh spacing that governs the localization response when a rate independent material model is used. For added accuracy and numerical stability, the constitutive model may also need to be modified to include viscosity, initial, and deformation-induced anisotropy, as well as other effects. Such model modifications are outside the scope of this paper. In our study, standard assumptions of isotropy, isotropic hardening, constant volume plastic deformation, and radial return plasticity, are used, and only the strain rate dependency has been investigated for its influence on the crash simulations. It is assumed that accurate strain fields are readily available for the evaluation of constitutive material models. Nevertheless, numerical simulations will illustrate some of the issues of

modeling of localized deformation and their interaction with the material model.

Determining the strain rate dependent properties of steel has not been a simple proposition. The range of strain rates in automotive impact span several orders of magnitude (i.e. 10^{-3} /s to 10^{+3} /s) [9]. One of the principal difficulties is interpretation and reconciliation of the data obtained from different experimental apparatus. In addition, the material properties in the strain rate orders of magnitude between 10^{+1} /s and 10^{+2} /s have been very difficult to obtain [9-12]. Interestingly enough, this is the range where important vehicle crash events take place [12]. New experimental equipment for this range has been recently developed [11]. It revealed the importance of material effects that were not considered in crash modeling before. In addition, new structural tests [13, 14], accompanied by FEM models have shown how structural experiments can be used for material characterization for the deformation modes of interest. Direct, coupon-level, experimental investigation of the strain rate dependency under generalized states of stress is still not practically possible, and structural tests combined with the FEM modeling are likely to provide sufficient information for the current modeling practices.

The paper is organized as follows. In the next section, general discussion on progressive crushing of tubular components is presented. Then, the current state of affairs in material modeling of strain rate effects in automotive crash is reviewed. The focus of the paper is on modeling of strain rate effects using the material model based on piecewise linear plasticity because of its prevailing use in automotive practice and its flexibility of representation of complex material behavior as a function of strain and strain rate. The following section deals with effects of strain rate sensitivity and material modeling approaches on simulated plastic strains and strain rates in the axi-symmetric tube crush. Next, non-symmetric crushing of circular tubes in drop tower experiments for High Strength Low Alloy (HSLA) and Dual Phase (DP) circular tubes is modeled and compared to the experimental results. The range of strains and strain rates from crush simulations, is summarized in conclusions.

MODELING OF DEFORMATION IN TUBE CRUSHING

The response of metals under multiaxial states of stress and varying strain rates is still far from being described by a unified theory. During multi-axial, large plastic deformation, material undergoes significant changes of microstructure and texture [1, 15] that lead to changes in material properties on the macroscopic level. From a practical standpoint, the goal is that the selected material model is applicable to the range of loading and deformation for the problem at hand. In tubular crush devices that are used as energy absorbers in vehicles,

metallic sheets are subjected to large, localized deformations that organize into global collapse mechanisms [16]. For a long time, analytical and semi-analytical methods [see reference 16 for review] were the only feasible routes for analyzing progressive structural collapse. The methods start from simplifying kinematics assumptions and idealization of material response, and derive the expressions for the structural response based on energy minimization principles. The advances in FEM and computational power have provided a framework where constraints of analytical approaches can be largely eliminated, and far more complex deformation and material responses can be modeled.

The standard practice for extracting strain rate relevant material parameters is to perform experiments with uniaxial loading configurations [17, 18]. The ductility of uniaxial tensile loaded specimens is limited by the geometric instability. For automotive steel sheets the magnitude of uniform plastic strains is limited to about 20%. However, the strains that are measured [13, 14] and modeled [19] during tube crushing far exceed this limit. The physical reality of large deformations is not in question [19]. The biaxial loading and bending provides additional stability that allows the utilization of a material's strain hardening, ductility and correspondingly large energy dissipation. The magnitude and distribution of plastic strains, large curvatures, and shifting of the neutral axis during fold formation clearly places the problem into the realm of large deformations.

Modeling of tube folds is the area where material models and finite element formulations are intrinsically linked. When shell elements are used to model tube crush, the issue of finite element resolution comes down to the number and type of bi-linear shell elements [20] that are used for modeling of a plastic fold. The experimentally measured curvature of full plastic folds is of the order of the material thickness. For the fold representation to be accurate, the element length should approach the shell thickness. It is at this point that the assumptions of the standard shell theory are stretched beyond their limits [19] and material models extrapolate far outside the experimentally verified range. On the other end of the spectrum, when the finite element resolution is fairly coarse (of the order of kinematic elements in analytical models), the material model extrapolation into large strains is not a concern because the strains get smeared over larger volumes and are within the range of uniaxial experimental data. However, the kinematics of the deformation are compromised.

In both of the above FEM meshing scenarios, in order to match the experimental results with models, material model parameters are commonly modified in engineering simulations. While the practice may be appalling to material scientists, the justification for

modification in one case is to compensate for the inability to represent local deformations and, in the other, to account for the significance of the large strain region for which experimental data is not available. The flexibility of computer programs now even provides methods for definition of optimization problems where the material parameters are determined so that they result in the optimal match between simulations and experiments [21] for crush measures such as impact force history and deceleration. These approaches are linked to specific structural problems, FEM mesh configurations and loading situations. A more rigorous approach would be to make sure that the FEM element resolution and element formulations are sufficient for accurate kinematic representation of the problem and then focus on compatible material modeling approaches.

MATERIAL MODELS FOR STRAIN RATE SENSITIVITY

Currently, the most commonly used approach to modeling strain-rate sensitivity in progressive crushing is to use isotropic plasticity models with a rate sensitivity component that has moderate requirements on the experimental program. The models that are frequently used for tube crush simulations are the Johnson-Cook model [22], the Zerilli-Armstrong model [23] and the piecewise linear strain rate sensitive material model [24]. The models are appealing because they have been implemented in commercial codes used for crash simulations and have a limited (≤ 6) number of material parameters that must be determined by experiments.

The strain rate sensitivity of BCC materials is attributed to the rate-controlling mechanism of the thermal component of the flow stress [1]. Since the activation volume for BCC metals is considered to be constant, the increase in strain rates should theoretically be described by an upward translation of the quasi-static strain-stress curve. Experimental results for mild and HSS show that the strain hardening rate decreases with an increase in strain rate, and the case of constant hardening rate can be viewed as a limiting case. Johnson-Cook material model is expressed in multiplicative form of strain, strain rate and temperature terms:

$$\sigma = (A + B\dot{\epsilon}^n)(1 + C \ln \dot{\epsilon})(1 - T^{*m}) \quad (1)$$

where A, B, C, n, and m denote material constants, and T^* is homologous temperature. The consequence of the multiplicative form is that the strain hardening rate at a certain strain will increase when the strain rate increases. The strain-stress curves for increasing strain rates will tend to “fan out” [25] which is in contrast to the experimental results for steel sheets. The material parameters can be selected such that strain hardening variations are insignificant. However, the model still cannot accommodate the global trend of reduction of

strain hardening rate with increasing strain rate. Mehadevan et al. [4] reported that the Johnson-Cook model gave better results than the Zerilli-Armstrong in the crush analysis although the assertion was linked to the element resolution and fit of the material model to the specific regions of experimental data. Their results illustrate a complex interplay between mesh resolution, deformation and dominant ranges of strain and strain rates.

Zerilli-Armstrong model for BCC metals is written in additive form akin to standard materials science expression for flow stress as an aggregate of various strengthening mechanisms:

$$\sigma = C_0 + C_1 \exp(C_3 T + C_4 T \ln \dot{\epsilon}) + C_5 \dot{\epsilon}^n \quad (1)$$

where C_i and n denote material parameters, and T is the absolute temperature. The strain hardening in the Zerilli-Armstrong model is constant across the strain rates and, therefore, the corresponding strain stress curves are parallel. The correlation of yield stresses [4, 25] with the Zerilli-Armstrong model has shown to be very good. However, the inherent inability to model the dependence of strain hardening on strain rate will unavoidably lead to adjustment of the element discretization and selection of specific strain intervals for material parameter derivation as it does for the Johnson-Cook model. The above focus on strain hardening is due to its crucial role in development of collapse pattern and bifurcation between crush modes [26]. Material models such as Bodner-Partom [27] and Khan-Huang [28] can offer added flexibility for modeling of strain hardening but they have not yet been widely implemented in commercial crash codes.

The most commonly used strain rate dependent material model in automotive engineering practice is the piecewise linear plasticity model. The model was used in this study because of its relevance to automotive crash modeling and flexibility for representation of strain rate sensitivity. In this approach, effective strain-stress curves are directly fed into the material models and require the least amount of effort for material model development. In simulations, for a given rate of strain (total or plastic), the resulting stress in the plastic region is linearly interpolated between the stress-strain values that were experimentally determined in strain rate tests. The blessing and the curse of this approach is that the model fits experimental data exactly, and that whatever testing artifacts or errors are contained in the experimental data will be carried over to the simulations. The highest strain rate in the experimental data acts as a saturation plateau for strain rate effects. Typical experimental true plastic strain-stress data for various strain rates for DQSK steel were developed by the Auto/Steel Partnership [29] and are shown in Figure 1:

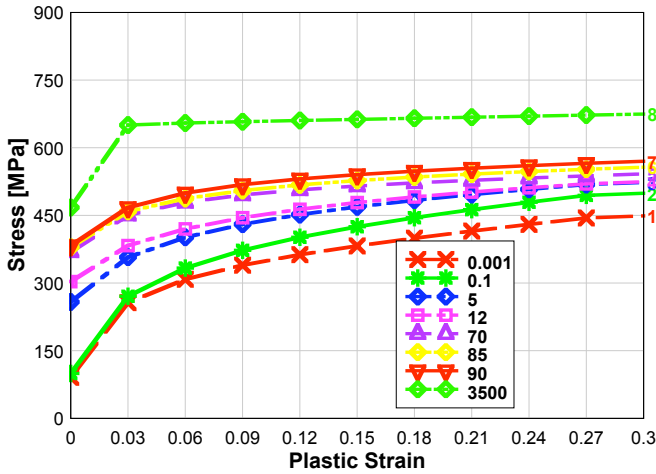


Figure 1. DQSK material data.

Important aspects of implementation of the piecewise linear plasticity model are the maximum strain rate for which the stress-strain data should be tested, and the number and arrangement of curves across the strain rate range. The data in Figure 1 contains all the available curves. The material model uses linear interpolation between the curves whereas it has been shown that the stress increment relation is logarithmic [30]. In the case when sufficient experimental data is available, the effects of linear interpolation should not be significant. Later in the article, it will be shown that adding logarithmically interpolated curves improves the model accuracy when experimental data is not available for the intermediate strain rates of 10^{+2} /s magnitudes. As also shown later, maximum calculated strain rates for crashworthiness simulations are of the order of 10^3 /s so that an experimental strain rate of that order would suffice as an upper rate limit for the model.

MODELING OF STRAINS AND STRAIN RATES IN AXISYMMETRIC CRUSHING OF STEEL TUBES

The objective of our study on axisymmetric crushing was to investigate the trends and magnitudes in plastic strains and strain rates as calculated by the finite element program. As stated above, this information is important in deciding the extent of the experimental program for derivation of material models.

A simulation of a typical axi-symmetric tube crush experiment is shown in Figure 2. A tube is clamped on the bottom and is impacted on the top with a moving mass. The experimental configuration from Reference 31 was used. The tube is made of mild steel that is modeled using a piecewise linear plasticity model with strain rate tabulated curves as shown in Figure 1. Tube thickness is 1.2 mm, radius 28 mm, and tube length is 180 mm.

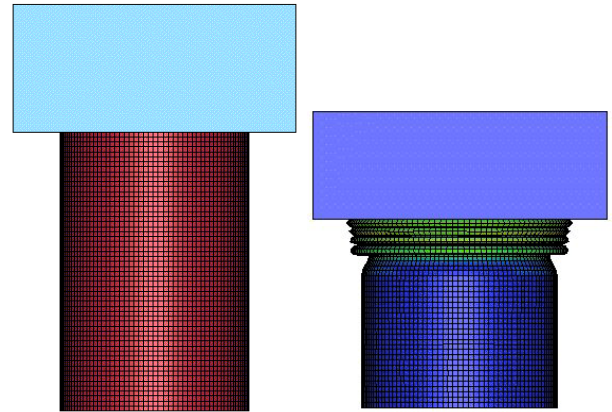


Figure 2. Tube crush test.

Due to the axial symmetry, the problem can be simplified by modeling a radial segment of the tube. The tube is modeled by a 2-degree wide cylinder segment with symmetry boundary conditions imposed on the radial sides. This results in a characteristic shell element length in the circumferential direction of 0.98 mm that is less than the tube thickness, so that the computational time increment will remain the same across different tube discretizations. Figure 3 shows the deformed tube segment for simulations using material with and without strain rate sensitivity. It is clear that the material strain rate sensitivity has a significant effect on the overall shortening of the tube.

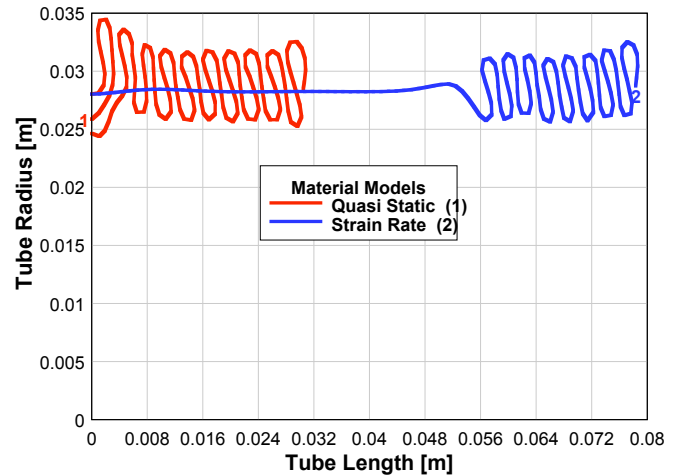


Figure 3. Deformed tube segment.

ELEMENT DISCRETIZATION

In order to investigate the effect of the FEM element discretization on the deformation and strain distribution we performed simulations with 23, 46, 92 and 160 elements. The length of an element in the 23-element configuration corresponds to the half-length of the fold in analytical models [16]. Figure 4 shows the final deformation of the tube for different element

discretizations. For the case when 23 elements are used across the tube length, the FE mesh is apparently too coarse to describe the resulting crush mode. As a consequence, when the entire circumference of the tube is modeled, the crush mode will not be axisymmetric or regular. For the case when 46 elements are used along the tube length, the general features of the crush are acceptable but the folds do not have smooth geometry. For 92 and 160 elements the deformation is smooth and in the agreement with the fold features from the experiments.

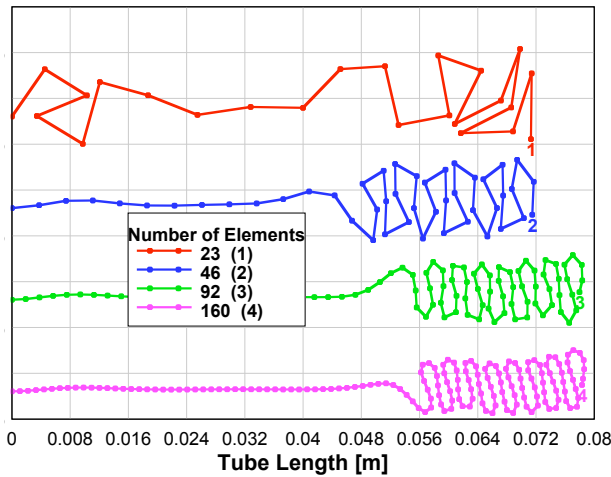


Figure 4. Deformed configurations for different FEM element discretizations

The effect of element discretization is better illustrated when the shell directors are analyzed. Figure 5 shows the deformed configurations for increasing mesh density together with the respective shell directors. The two coarsest meshes have large rotations of the directors that lead to poor description of strain fields.

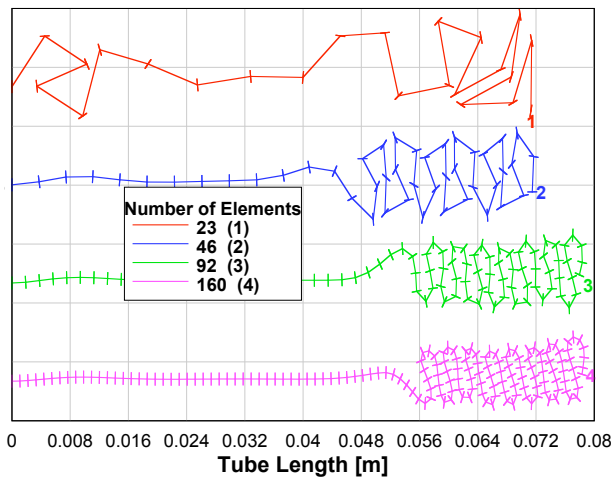


Figure 5. Shell directors for different element discretizations

In the case when 160 elements along the length are used, the element length is of the order of element thickness. Experimentally measured curvature of the tube fold is also of the same order. The curvature distributions along the undeformed length of the tube for different element discretizations are shown in Figure 6.

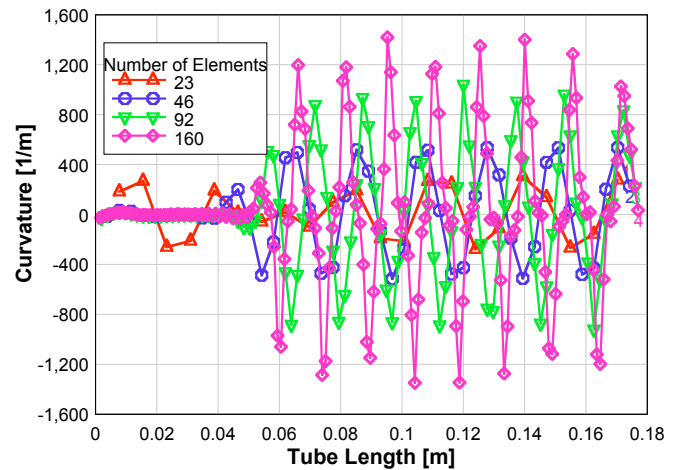


Figure 6. Curvature of the tube for different element discretizations

STRAIN RATES

Crashworthiness simulations are almost exclusively done using FEM programs with explicit time integration [24]. The explicit time integration algorithms are only conditionally stable, which means that the integration time step must be smaller than the time for a disturbance to travel across the smallest finite element in the model. For example, for steel and a finite element characteristic length of 5mm, this condition requires that the time step be smaller than 1 microsecond. The material constitutive relations and strain rates are calculated at this smallest time scale where wave propagation effects are important. The experimental data are determined on the higher time scales where the wave effects are not measured except for the experiments with highest rates. Therefore, it is important to determine the values of the strain rates in the explicit time integration calculations in order to define the extent of the required material experimental characterization program. It is also important to investigate the effects of FEM formulations and element discretization on magnitudes and distribution of plastic strains and strain rates in the areas of large plastic deformations that determine the crush mode, since these can then be correlated to the tube crush experiments [14].

The simulations show the clear dependence of the strain rate calculations on the element discretization. Characteristic plastic strains and plastic strain rates for different element discretizations at the time of formation of the second fold are shown in Figures 7 and 8.

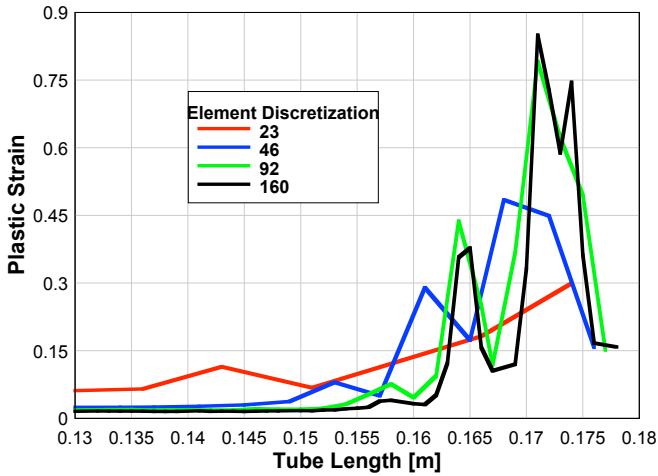


Figure 7. Maximum plastic strain distribution mapped on the original tube length

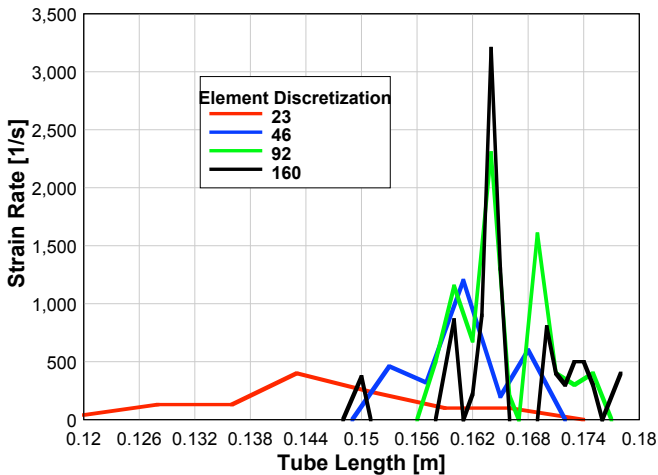


Figure 8. Maximum plastic strain rate distribution mapped on the original tube length

Contrary to the plastic strains that tend to monotonically increase, strain rates exhibit intermittent bursts of activity in the area of evolving plastic folds. The strain and strain rate distributions for the 92 and 160 element discretization seem to stabilize in magnitude and distribution. The maximum strains are slowly changing in time while strain rate curves violently oscillate as a result of passing disturbance waves in the structure [8] and the material model that is based on total strain rate.

When the material model uses plastic strain rate [32] as the basis for stress calculation (VP=1 in the LS-DYNA3D parlance), the dynamics of strain rate distribution drastically change. The strain rates in the model are oscillating much less compared to the situation where total strain rate is used. This is illustrated in Figures 9 and 10, respectively. The figures show the sequences of strain rate distributions for 92 element mesh for ten time instances around 3 ms simulation time that are about

five computational time increments apart. The shade of grey for the curves denotes the time sequence in the increasing order. For a material model based on total strain rate in Figure 9, strain rate distributions vary significantly, whereas in Figure 10 the variation in strain rate history is much more gradual.

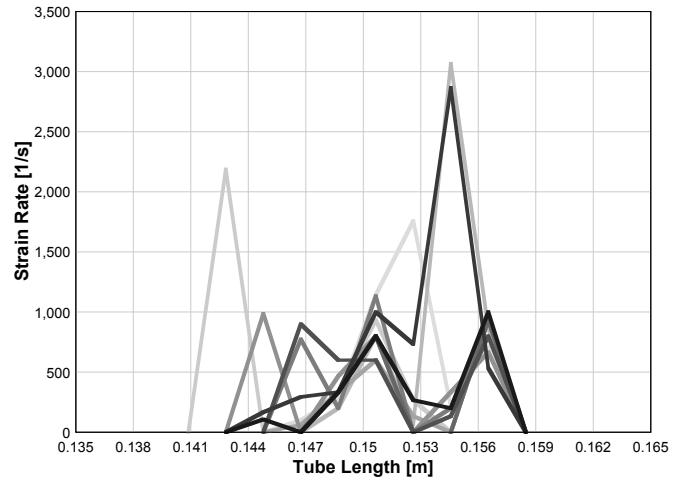


Figure 9. Strain rate history for material model based on total strain rate

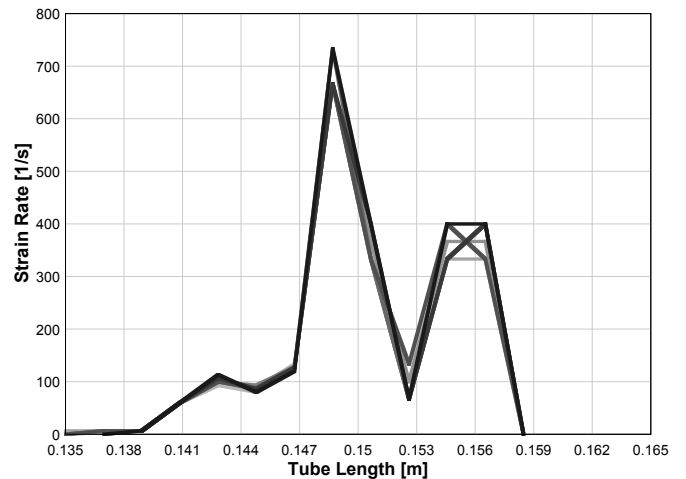


Figure 10. Strain rate history for material model based on plastic strain rate

The strain rate history from the model based on plastic strain rate in Figure 10 appears to be more physically realistic than the one for the model based on total strain rate. In the case of the plastic strain based model, the strain rates are more gradually changing throughout the simulation, and have strain rate magnitudes that rarely exceed the experimentally available values.

HSS CIRCULAR TUBE CRUSH EXPERIMENTS

Although notorious for its imperfection sensitivity [33, 34] and abundance of crush modes of seemingly identical energy [35], circular tube crushing can be used not only

to verify the modeling methods but also to investigate the important material properties. The in-depth review of the experimental procedures for buckling of thin tubular structures can be found in recent monographs on the subject [33, 34].

In this project, HSS materials HSLA350 and DP600 were selected for drop tower experiments in order to investigate the accuracy of the constitutive models based on piecewise linear plasticity model and various modeling approaches. The tests were modeled before the actual physical experiments to determine the test parameters. A test configuration for the HSLA350 steel tube and the final deformed shape are shown in Figures 11 and 12. The tube with radius of 50 mm, thickness of 1.6 mm and the length of 160 mm, was welded to the base plate, which was bolted to the test fixture, and the drop weight of 315 kg impacts the tube at 6.39 m/s. Force, accelerations, and high-speed photographs were recorded during the experiments.



Figure 11. Test configuration



Figure 12. HSLA350 tube at the end of experiment

Characteristic force-time traces from HSLA350 tube crush experiment for two tests are shown in Figure 13.

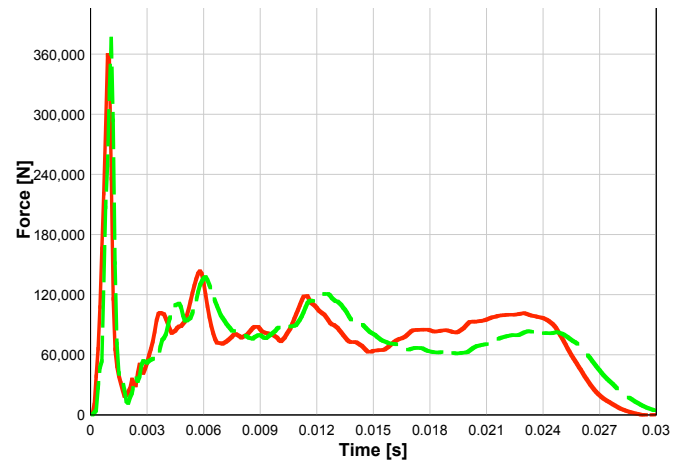


Figure 13. Force history for HSLA350 tubes

The force-time diagram shows the characteristic peak followed by the force plateau associated with progressive tube folding. The HSLA350 tubes deformed in an anti-symmetric, triangular pattern. The anti-symmetric modes are principal mechanisms of deformation for the tube dimensions and the ranges of imperfections considered.

The deformed shape of the DP600 tube is shown in Figure 14. The tube radius was 40 mm, tube thickness was 1.24 mm and the length was 120 mm. The weight of 315 kg and impact velocity of 5.6 m/s were selected to completely crush the tube without contacting the honeycomb stoppers. The corresponding force-time diagram for three samples is shown in Figure 15.



Figure 14. DP600 tube at the end of experiment

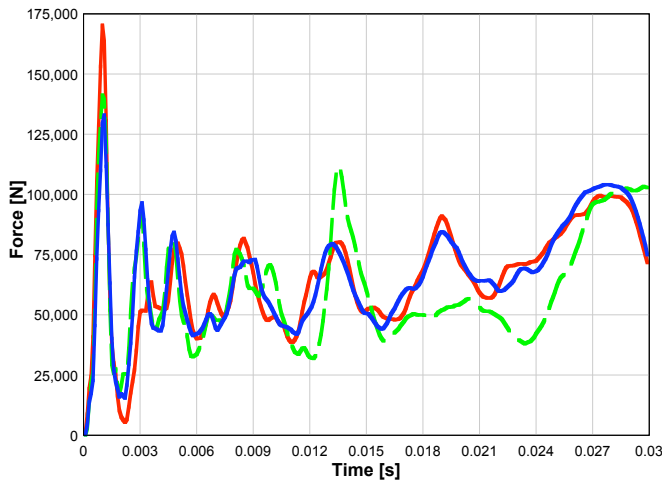


Figure 15. Force history for DP600 tubes

Similarly to the HSL350 tubes, the initial force peak is followed by the oscillations characteristic of the progressive crushing.

PIECEWISE LINEAR PLASTICITY MODEL FOR HSLA AND DP STEELS

Data from several testing methods has been used to develop the model parameters. The strain-stress curves for different rates are shown in Figures 16 and 17 for HSLA350 and DP600 materials, respectively.

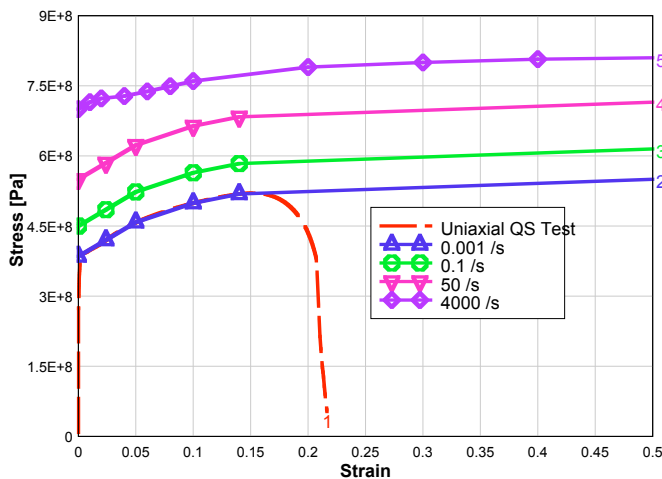


Figure 16. Material parameters for HSLA350

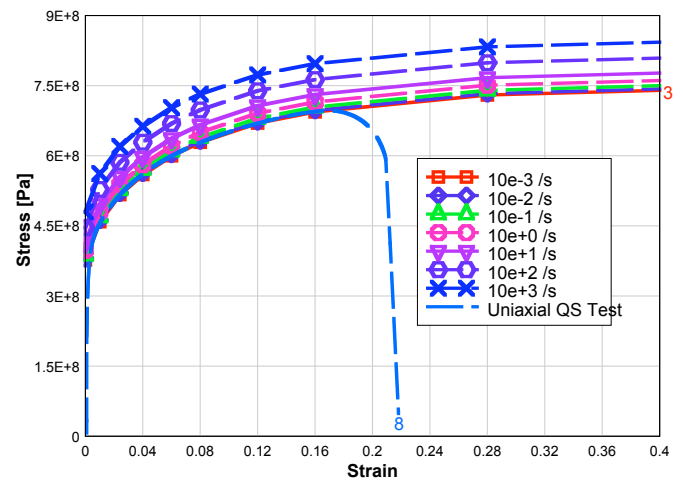


Figure 17. Material Parameters for DP600

The DP600 material has lower strain rate sensitivity compared to HSLA350. Also, the information for all strain rate levels of magnitude between the minimum and maximum levels for HSLA350 was not always consistent, and only the non-conflicting information has been used in the model. That resulted in having only stress-strain curves for strain rates of 50 /s and 4000 /s. However, it was shown in this study (see Figures 9 and 10) that the strain rate magnitudes of 10^{+2} /s are prevalent in for the impact situations and mesh resolutions of interest. It was also shown that adding more stress-strain curves using logarithmic interpolation to strain rate magnitudes of 10^{+2} /s and 10^{+3} /s yields more accurate results and a smoother strain rate distribution history. In Figures 16 and 17, dashed curves show the results from the quasi-static uniaxial tensile experiments on material cut from the actual tubes.

IMPACT SIMULATIONS

Because of the imperfection sensitivity of circular tubes it was necessary to incorporate imperfections into the models. The various modes and magnitudes of imperfections were considered to determine the controlling factors for tube fold formation. The main purpose was to investigate the relative influence of the various types of imperfections that were present in the tubes on the crush behavior. It was determined that the tube height (or equivalently the loading plate angle) have dominant influence on tube crush for the imperfection ranges in the tubes. This finding is agreement with experiments reported in the literature [36]. For a perfect tube and perfect loading conditions, the model predicts that the tube deforms by several axi-symmetric folds before it bifurcates into an anti-symmetric pattern. However, in the real world, imperfections are always present, and tubes quickly bifurcate into anti-symmetric modes. The tubes were modeled using fully integrated shell elements (shell type 13 in LS-DYNA3D) with element size equal to 1.9 element thicknesses. The

comparison of the HSLA350 drop tower model with characteristic imperfections and the experiment is shown in Figure 18.

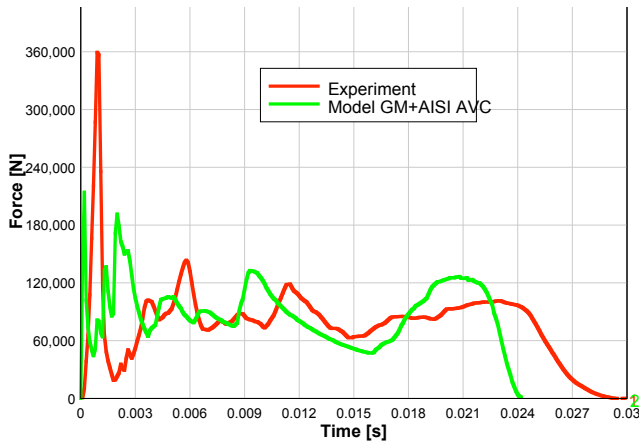


Figure 18. HSLA350 Drop Tower Simulation

The model for the HSLA350 tube underestimates the initial peak of the impact force. The remaining process of tube crushing shows relatively good agreement with the test. The initial increased flexibility of the system in the experimental data is a result of the details of the experimental setup (trigger strip, plywood and steel plate sandwich on drop mass) that were not included in the model. Figure 19 shows the force time diagram comparison for the DP600 tube. In this case, the model gives a good estimate of the initial force peak.

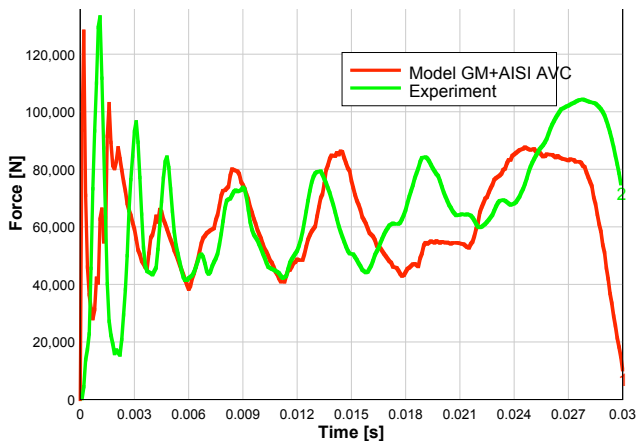


Figure 19. DP600 Drop Tower Simulation

The possible reasons for the model discrepancy in the ability to model the force peak in the two different materials can be a result of different strain hardening in the materials and the lack of modeling upper and lower yield point [37] in the HSLA350 tubes. The predicted tube collapse shape for HSLA350 tubes is shown in Figure 20. The folding pattern is square whereas the tests exhibited the triangular pattern.

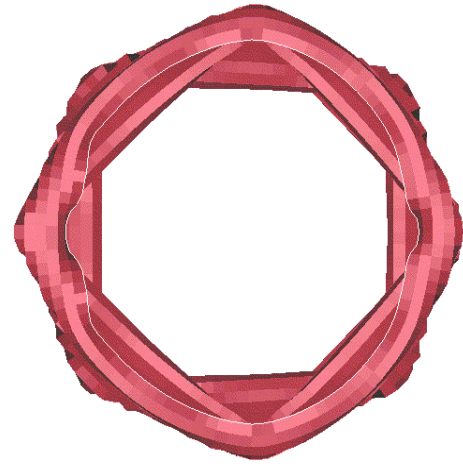


Figure 20. Folding pattern for original material model

When the HSLA350 material model was modified by using viscoplasticity option and adding logarithmically interpolated strain-stress curves for in 10^{+2} /s range, a triangular folding shape was obtained (Figure 21).



Figure 21. Folding pattern for material model with logarithmically interpolated material data

The fact that the crushing modes have been changed illustrates the effect of details on modeling of structural collapse. The crush modes in circular tubes are very close and different modes in simulations can also be influenced by other modeling factors (even more so than by the material model), such as shell element formulation, FE mesh resolution, viscoplasticity option, etc. However, the simulations indicate that the peak force is directly related to the material model and the magnitude of imperfection. In the above HSLA350 tube crush simulation, the simulated peak force was still lower than the experiment. Current research is looking at the effect of adding upper and lower yield behavior in the material models. Recent tests performed in the mid and high strain rates show pronounced upper and lower yield

points for some steels [11, 18, 29]. The existence of this effect in HSLA steels has not been clearly established but the above discrepancy seems to be supporting such a premise. These results also support the premise that material properties at strain rates in the 10^{+2} /s range are very important for modeling of progressive tube crushing in automotive applications.

CONCLUSIONS

An improvement in predictive capability of the crashworthiness models is linked to development of realistic material models and finite elements with better representation of complex strain and stress states in progressive crushing. Strain rate sensitivity is an important component of the material models and needs to be incorporated in the crashworthiness models. The paper reports on the range of strains and strain rates calculated in the explicit FEM programs that are used for evaluation of constitutive models. Strain rate magnitudes of the order of 10^{+3} /s provide a reasonable upper limit for the model. Strain rate magnitudes of the order of 10^{+2} /s are prevalent for shell element sizes that are of the order of 1-2 tube shell thicknesses. The viscoplastic option for material modeling provides more realistically feasible strain rate histories. For modeling details of tube crushing, the FEM mesh discretization should be fine enough, as measured by the strain distribution, angle of shell directors, and resulting curvature, to model the crush fold formation. Once the kinematics are accurately approximated, the material model can be investigated for possible indications of material properties in the range where the experimental coupon tests are difficult to conduct. Current results indicate a close link between the strain rate calculations and element type and discretization, and will be analyzed in more detail in the following publications.

ACKNOWLEDGMENTS

Research was sponsored by the U.S. Department of Energy, Assistant Secretary for Energy Efficiency and Renewable Energy, Office of Transportation Technologies, Lightweight Materials Program, under contract DE-AC05-00OR22725 with UT-Battelle, LLC. The support of Auto/Steel Partnership Strain Rate Characterization Team is acknowledged. The tests were performed at the Vehicle Safety and Crashworthiness Laboratory, General Motors Corporation, Milford Proving Grounds.

CONTACT

For additional information on details on the research project please contact Srdan Simunovic, simunovics@ornl.gov. Dr. Simunovic is a senior research staff in the Computational Materials Science

Group (<http://www-cms.ornl.gov>) at the Oak Ridge National Laboratory.

The submitted manuscript has been authored by a contractor of the U.S. Government under contract No. DE-AC05-00OR22725. Accordingly, the U.S. Government retains a nonexclusive, royalty-free license to publish or reproduce the published form of this contribution, or allow others to do so, for U.S. Government purposes.

REFERENCES

1. Constitution and Properties of Steels, vol. ed. Pickering, F. B., Materials Science and Technology, vol. 7, VCH, New York, 1992.
2. Manjoine, M.J., Influence of rate of strain and temperature on yield stresses of mild steel", J. Appl. Mech. vol. 11 p. 211-218, 1944.
3. Campbell, J. D., Dynamic Plasticity of Metals, Springer, New York, 1972.
4. Mahadevan, K., Fekete, J. R., Schell B., McCoy, R., Faruque, O., Strain-Rate Characterization of Automotive Steel and the Effect of Strain-Rate in Component Crush Analysis, SAE paper 982392, 1998.
5. Mahadevan, K., Fekete, J. R., Liang, P., Effect of Strain-rate in Full Vehicle Frontal Crash Analysis, SAE paper 2000-01-0625, 2000.
6. Simunovic, S., Shaw, J., Aramayo, G., Material modeling effects on impact deformation of ultralight steel auto body, SAE Paper 2000-01-2715, 2000.
7. Needleman, A., Material rate dependence and mesh sensitivity in localization problems. Computer Methods in Applied Mechanics and Engineering, vol. 67, no.1, p. 69-85, 1988.
8. R. J. Clifton, Plastic waves: Theory and experiment, in S. Nemat-Nassser, ed., Mechanics Today 1, p. 102-167, 1974.
9. Bleck, W., Schael, I., Determination of crash-relevant material parameters by dynamic tensile tests Steel Research, vol. 71, no. 5, p 173-178, 2000.
10. Valentin, T., Magain, P., Quik, M., Labibes, K., Albertini, C. Validation of constitutive equations for steel. Journal de Physique IV (Colloque), vol.7, no. C3, p.611-616, 1997.
11. Hove, I.H., Andersson, B., Johnsen, T.E. High speed tensile testing. Journal de Physique IV (Colloque), vol.7, no.C3, p.229-34, 1997.
12. Hira, T., Hiramoto, J., Sakata, K., Utilization of finite element method for expanding application of high strength steels for automotive body, Kawasaki Steel Technical Report, no. 46, p.12-18, 2002.
13. Tam, L.L., Calladine, C.R., Inertia and strain-rate effects in a simple plate-structure under impact loading International Journal of Impact Engineering, vol. 11, no. 3, p 349-377, 1991.
14. Avalue, M., Belingardi, G., Experimental evaluation of the strain field history during plastic progressive folding of aluminium circular tubes International Journal of Mechanical Sciences, vol. 39, no. 5, p 575-583, 1997.
15. Hansen, N., Huang, X., Hughes, D.A., Microstructural evolution and hardening parameters. Materials Science & Engineering A (Structural Materials: Properties, Microstructure and Processing), vol. A317, no. 1-2, p.3-11, 2001.
16. Jones, N., Structural Impact, Cambridge University Press, 1989.
17. Field, J.E., Walley, S.M., Bourne, N.K., Huntley, J.M. Experimental methods at high rates of strain. Journal de Physique IV (Colloque), vol.4, no. C8, p. C8/3-22, 1994.
18. Quik, M., Labibes, K., Albertini, C., Valentin, T., Magain, P. Dynamic mechanical properties of automotive thin sheet steel in tension, compression and shear. Journal de Physique IV (Colloque), vol.7, no. C3, p.379-384, 1997.

19. Triantafyllidis, N., Needleman, A., Tvergaard, V., On the development of shear bands in pure bending. *International Journal of Solids and Structures*, vol.18, no.2, p.121-138, 1982.
20. Galbraith, P.C, Hallquist, J.O., Shell-element formulations in LS-DYNA3D: their use in the modeling of sheet-metal forming, *Journal of Materials Processing Technology*, vol. 50, no. 1-4, , p 158-167, 1995.
21. Markiewicz, E., Ducrocq, P., Drazetic, P., Inverse approach to determine the constitutive model parameters from axial crushing of thin-walled square tubes, *International Journal of Impact Engineering*, vol. 21, no. 6, 1998,
22. Johnson, G. R. and Cook, W. H., A Constitutive Model and Data for Metals Subjected to Large Strains, High Strain-rates and High Temperatures, *Proceedings of the Seventh International Symposium on Ballistic*, Hague, Netherlands, p. 541-547, 1983.
23. Zerilli, F. J. and Armstrong, R. W., Dislocation-Mechanics-Based Constitutive Relations for Material Dynamics Calculations," *Journal of Applied Physics*, vol. 61, no. 5, p. 1816-1825, 1987.
24. Hallquist, J. O., LS-DYNA3D, An explicit finite element nonlinear analysis code for structures in three dimensions, LSTC Manual, 1995.
25. Liang, Riqiang, Khan, Akhtar S., Critical review of experimental results and constitutive models for BCC and FCC metals over a wide range of strain rates and temperatures, *International Journal of Plasticity*, vol. 15, no. 9, p 963-980, 1999.
26. Tvergaard, V. On the transition from a diamond mode to an axisymmetric mode of collapse in cylindrical shells. *International Journal of Solids and Structures*, vol. 19, no. 10, p.845-856, 1983.
27. Bodner, S.R., Partom Y., Constitutive equations for elastic-viscoplastic strain-hardening materials. *Journal of Applied Mechanics*, p. 385-389, 1975.
28. Khan, A.S., Huang, S., Experimental and theoretical study of mechanical behavior of 1100 aluminum in the strain rate range 10⁻⁵ – 10⁴ s⁻¹ *International Journal of Plasticity*, vol. 8, 397-424, 1992.
29. <http://www.a-sp.org>
30. Davies, R. G. and Magee, C. L., The Effect of Strain-Rate Upon the Tensile Deformation of Materials, *Journal of Engineering Materials and Technology*, vol. 97, no. 2, p. 151-155, 1975.
31. Abramowicz, W. and Jones, N., Dynamic Axial Crushing of Circular Tubes, *Int. J. of Impact Eng.*, vol. 2, no. 3, p. 263-281, 1984.
32. Berstad, T., Hopperstad, O., Langseth, M., Elasto-viscoplastic constitutive models in the explicit finite element code LS-DYNA3D, In 2nd LS-DYNA Conference, 1994.
33. Singer, J., Weller, T., Arbocz, J., Basic Concepts, Columns, Beams and Plates, Volume 1, *Buckling Experiments: Experimental Methods in Buckling of Thin-Walled Structures*, John Wiley & Son Ltd., 1998.
34. Singer, J., Weller, T., Arbocz, J., *Buckling Experiments: Experimental Methods in Buckling of Thin-Walled Structures: Shells, Built-Up Structures and Additional Topics*, John Wiley & Son Ltd., 2002.
35. Calladine, C., *Theory of Shell Structures*, Cambridge Univ. Press, 1983.
36. Copa, A., Effect of end conditions on buckling of cylindrical shells under axial compression impact, In *Test Methods for Compression Members*, ASTM Tech. Pub No. 419, p.115-136, 1966.
37. El-Magd, E., Scholles, H., Weisshaupt, H., Influence of strain rate on the stress-strain curve in the range of Luders strain, *Steel Research*, vol. 67, no. 11, p. 495-500, 1996.